Acta geographica Slovenica, 66-1, 2026, 99–119

MAPPING AND ASSESSING FOREST FIRE SEVERITY USING REMOTE SENSING INDICES: A CASE STUDY OF TIZI OUZOU, ALGERIA

Boudjemline Fouzia

Forest fires in northern Algeria, including the Tizi Ouzou area, as seen in a Copernicus Sentinel-2 image captured on 12 August 2021. Image processed by ESA.

DOI: https://doi.org/10.3986/AGS.14459
UDC: 630*43:528.8(65-17)"2021"

Boudjemline Fouzia

Mapping and assessing forest fire severity using remote sensing indices: A case study of Tizi Ouzou, Algeria

ABSTRACT: In Mediterranean regions, wildfires are exacerbated by rising temperatures and drought, stressing the need for rapid post-fire evaluation. This study employs Landsat-8 imagery to evaluate the effects of forest fires during summer 2021 in Tizi Ouzou region, Algeria. We calculated the Normalized Burn Ratio (NBR) and its difference (dNBR) from pre- and post-fire images, and analyzed the Normalized Difference Vegetation Index (NDVI) and Land Surface Temperature (LST) to evaluate vegetation loss and thermal response. Results indicate 24,700 hectares (~6.7%) with high severity, 55,200 ha (14.9%) with moderate–high and 94,500 ha (25.5%) with moderate–low. These findings highlight the value of combining spectral and thermal indices for wildfire assessment, offering guidance for restoration and management.

KEYWORDS: wildfire, remote sensing, land surface temperature, NDVI, dNBR, Tizi Ouzou, Algeria

Kartiranje in ocenjevanje resnosti gozdnih požarov z uporabo indeksov daljinskega zaznavanja: študija primera Tizi Ouzou, Alžirija

POVZETEK: V sredozemskih pokrajinah so gozdni požari vedno resnejši zaradi naraščajočih temperatur in suše, kar poudarja potrebo po hitri oceni stanja po požaru. Ta študija uporablja posnetke Landsat-8 za oceno učinkov gozdnih požarov poleti 2021 v regiji Tizi Ouzou v Alžiriji. Izračunali smo normalizirano razmerje požarne prizadetosti (NBR) in njegovo razliko (dNBR) iz posnetkov pred požarom in po njem ter analizirali normalizirani indeks razlike vegetacije (NDVI) in temperaturo površine tal (LST), da bi ocenili izgubo vegetacije in toplotni odziv. Rezultati kažejo, da je bilo zelo prizadetih 24.700 hektarjev (~6,7 %), 55.200 ha (14,9 %) zmerno do zelo prizadetih in 94.500 ha (25,5 %) zmerno do malo prizadetih. Rezultati poudarjajo pomen kombiniranja spektralnih in toplotnih indeksov za oceno posledic gozdnih požarov, saj ponujajo smernice za obnovo in upravljanje.

KLJUČNE BESEDE: gozdni požar, daljinsko zaznavanje, temperatura površine tal, NDVI, dNBR, Tizi Ouzou, Alžirija

The article was submitted for publication on May 16th, 2025.
Uredništvo je prejelo prispevek 16. maja 2025.

[1] Teacher Education College of Setif (ENS), Setif, Algeria
f.boudjemline@ens-setif.dz (https://orcid.org/0009-0002-7071-962X)

1 Introduction

Forest fires, increasingly recurrent across Mediterranean regions due to climatic shifts, land-use changes, and socio-economic transformations (Ganteaume and Barbero 2019; Dupuy et al. 2020), are among the primary contributors to environmental degradation in the Mediterranean Basin. They particularly effect on soil structure, hydrological processes, and vegetative cover (Lovreglio et al. 2010). The removal of protective vegetation layers exposes soils to erosion and alters infiltration dynamics, thereby accelerating land degradation (Stefanidis et al. 2022). In this context, rapid and accurate post-fire damage assessment is essential to guide effective forest management, ecological restoration, and risk mitigation (Brewer et al. 2005).

In this study, we distinguish between »wildfires«, defined as any uncontrolled fire in natural areas, and »forest fires«, which specifically affect forested ecosystems, following Keeley (2009). Burn severity, defined as the magnitude of ecological change and land cover alteration caused by fire, reflects the degree to which vegetation and soil are affected. It can be quantified through different indicators, such as the percentage of area burned, the proportion of vegetation destroyed, or the decrease in spectral indices like NDVI (Keeley 2009; Cansler and McKenzie 2012). However, measuring burn severity presents considerable challenges due to the complexity of fire effects and the heterogeneity of impacted landscapes (Cocke et al. 2005). Remote sensing technologies have emerged as effective tools in this domain, offering synoptic coverage and temporal consistency across vast and often inaccessible terrains. Their effectiveness in wildfire monitoring and burn severity assessment has been widely demonstrated in recent studies (Durlević et al. 2025; Sabljić et al. 2025). Spectral indices such as the Normalized Difference Vegetation Index (NDVI) and the Normalized Burn Ratio (NBR) are widely used to evaluate vegetation loss and fire impacts, both of which are directly related to burn severity (Harris et al. 2011). More recently, Land Surface Temperature (LST) has gained attention for its potential to reflect burn severity, as post-fire environments typically exhibit elevated temperatures due to reduced evapotranspiration and increased surface heat flux (Wendt et al. 2007; Veraverbeke et al. 2010; Vlassova et al. 2014).

Over the past two decades, catastrophic wildfires have repeatedly struck the Mediterranean – including France (2003), Greece (2007), Portugal (2017), Algeria, Turkey, and Greece (2021) – and across southern Europe in 2022, when nearly 900,000 ha burned (Mouillot et al. 2003; Turco et al. 2019; Koutsias et al. 2022; San-Miguel-Ayanz et al. 2022). These events underscore the region's vulnerability linked to climate variability, land-use change, and socio-economic pressures (Lukić et al. 2017; Vujović et al. 2024). These events reveal a critical research gap: while numerous studies have examined fire impacts in the Mediterranean, few have integrated thermal parameters such as LST with spectral indices (e.g., dNBR) to assess burn severity. This study is the first to systematically apply these indices to the Tizi Ouzou region using Landsat 8 imagery, providing new insights for regional wildfire management and contributing to improved post-fire assessment methodologies.

In Algeria, over 36,000 hectares of forest are destroyed by wildfires each year (Direction Générale des Forêts 2021). The economic losses in the forestry sector caused by these fires between 1985 and 2006 were estimated at over 113 billion Algerian dinars (approximately 1.11 billion euros) (Arfa et al. 2019). This financial assessment considers only the market value of the lost products – such as timber, cork, scrubland, esparto grass, and fruit trees – without accounting for the annual expenditures dedicated to firefighting efforts. In more recent years, Algeria has faced an escalating wildfire crisis, with the 2021 fire season alone recording 1,631 incidents that devastated approximately 100,101 hectares of vegetation (Direction Générale des Forêts 2021). These events were exacerbated by unprecedented heatwaves and prolonged droughts, trends that align with regional projections under current climate change scenarios.

Remote sensing analyses over the past four decades have revealed that approximately 81% of burnable land in Tizi Ouzou has experienced wildfires between 1984 and 2023, with over half of these zones subjected to repeated burns (Kouachi et al. 2024). This chronic recurrence illustrates the ecological pressure on Mediterranean landscapes. Researchers increasingly use GIS and statistical modeling to map fire-prone zones and inform prevention strategies (Oliveira et al. 2012; Rahmani and Benmassoud 2019; Lahmar and Akakba 2024; Castro-Melgar et al. 2025). These tools underscore the necessity of integrating local ecological conditions with community-based awareness and mitigation programs (Belgherbi et al. 2018).

The present study builds upon previous advances in wildfire assessment using remote sensing and GIS, particularly the integration of spectral indices and thermal metrics, to evaluate the potential of LST as a reliable indicator of burn severity in the forested areas of Tizi Ouzou Province. Utilizing a multi-sensor remote sensing approach – particularly combining the dNBR, a spectral index derived from NIR and SWIR bands widely used to quantify burn severity, with LST, the radiative temperature of the land surface obtained from thermal infrared data – this research aims to generate a comprehensive spatial analysis of post-fire conditions in this Mediterranean hotspot. The study specifically explores how LST correlates with burn severity, and how pre-fire ecological factors, such as vegetation density and topographic variability, influence post-fire thermal responses.

Furthermore, geospatial tools will be applied to identify and prioritize high-severity zones for ecological restoration, evaluate site suitability for reforestation based on environmental criteria, and support the strategic allocation of fire management resources. The study also underscores the importance of community engagement in the design and implementation of rehabilitation efforts.

The present study addresses the following key research questions:

1. To what extent can Land Surface Temperature (LST) serve as a reliable indicator of burn severity in the forested areas of Tizi Ouzou Province?
2. How does LST correlate with the differenced Normalized Burn Ratio (dNBR) in assessing post-fire ecological transformations?
3. How can geospatial tools be applied to identify high-severity zones and support reforestation and fire management strategies?

By addressing these questions, this research aims to advance remote sensing methodologies for fire assessment and contribute to evidence-based ecological rehabilitation and policy development in Mediterranean Algeria.

2 Materials and methods

2.1 Study Area

The Tizi Ouzou study area is located in northern Algeria (Figure 1) and extends over approximately 2,958 km^2 between latitudes 36°30’–37°00’ N, and longitudes 3°30’–4°30’ E. Elevation ranges from 10 m in the coastal plains to 2,308 m at the Djurdjura Mountains, giving rise to a predominantly hilly and mountainous relief. Geologically, the region is composed of Cretaceous and Tertiary formations interspersed with recent alluvial

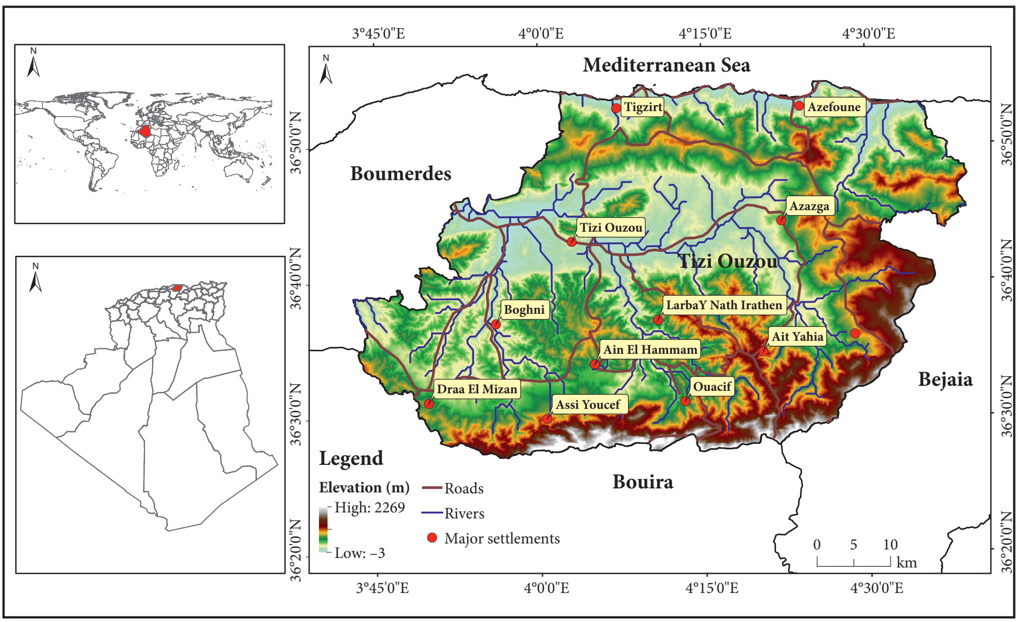

Figure 1: Study area map showing the location of the district of Tizi Ouzou.

deposits, while geomorphologically it is defined by rugged slopes, erosion-prone terrain, and valleys incised by rivers originating from the Djurdjura massif. Climatically, the area experiences a typical Mediterranean climate, characterized by hot, dry summers and mild, wet winters, with average annual precipitation ranging between 500 and 800 mm (Meddour and Derridj 2010). Forested land accounts for nearly 38% of the territory and is dominated by maquis shrublands) e.g., *Quercus coccifera, Pistacia lentiscus*) and coniferous stands of cedar (*Cedrus atlantica*) and Aleppo pine (*Pinus halepensis*) (Ammiche and Oumezzaouche 2018). The Tizi Ouzou province, encompassing ~112,180 ha of vegetated land, is highly vulnerable to wildfires due to dense forests, complex topography, and human pressures. Maquis vegetation occupies nearly half of the forest area, followed by state-owned forests, with smaller shares of reforested and communal lands (Conservation des forêts Tizi Ouzou 2021; Sahar et al. 2020). This ecological richness, however, is increasingly threatened by recurrent fires, many of which are linked to anthropogenic activities.

2.2 Data sources and methodology

The methodology adopted in this study is illustrated in Figure 2. Landsat-8 Operational Land Imager (OLI) and Thermal Infrared Sensor (TIRS) imagery were obtained from the United States Geological Survey Earth Explorer platform to assess wildfire impacts in the Tizi Ouzou region. Landsat-8, launched in 2013, is equipped with OLI and TIRS sensors that provide multispectral and thermal observations at spatial resolutions ranging from 15 to 100 m. These data enable detailed monitoring of vegetation dynamics, fire severity, and land surface temperature (Roy et al. 2014). The key characteristics of the Landsat-8 bands used in this study are summarized in Table 1.

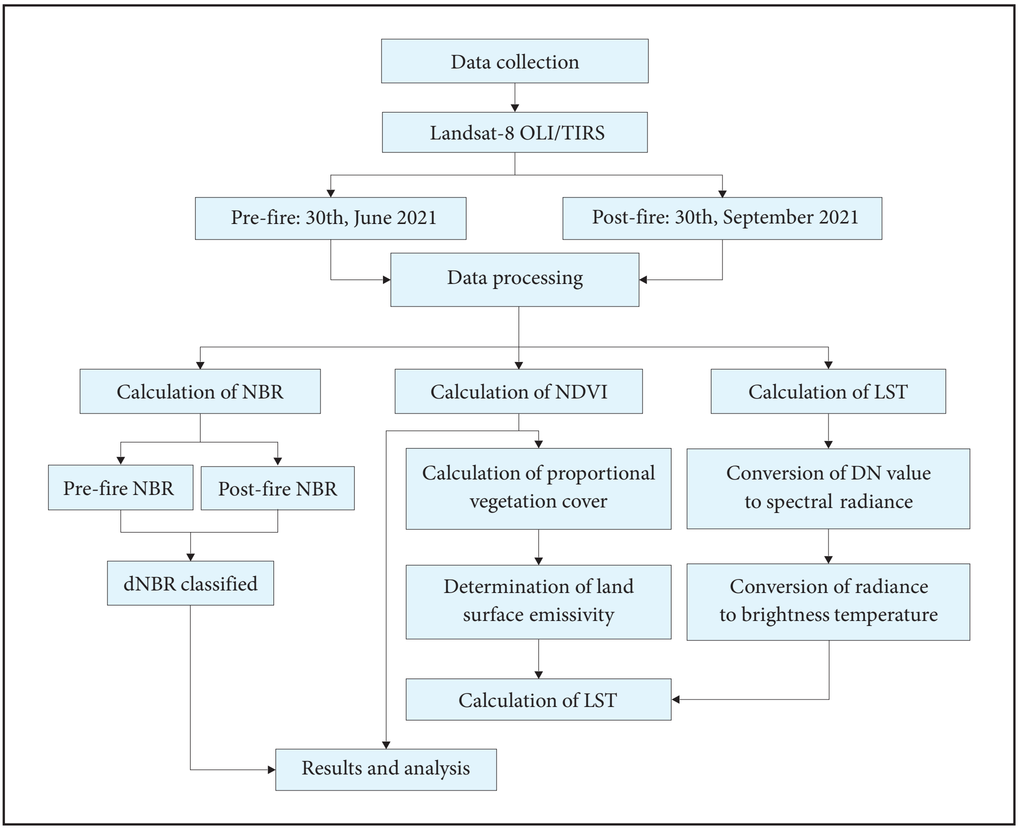

Figure 2: Flowchart illustrating the research methodology.

Table 1: Key characteristics of Landsat-8 OLI/TIRS data used in this study.

Band	Spectral region	Wavelengths (μm)	Resolution (m)	Sensor	Main applications
B4	Red	0.630–0.680	30	OLI	NDVI, NBR
B5	Near Infrared (NIR)	0.845–0.885	30	OLI	NDVI, NBR
B7	Shortwave Infrared-2	2.100–2.300	30	OLI	NBR
B10	Thermal Infrared	10.60–11.19	100 (resampled to 30)	TIRS	LST

Two cloud-free scenes were selected, dated 30 June 2021 (pre-fire) and 30 September 2021 (post-fire), corresponding to Path 193 / Row 35. These dates were chosen to bracket the major wildfire event that occurred on 9th August, 2021 and to best represent vegetation conditions immediately before and after the disturbance. Furthermore, according to Algerian National Office of Meteorology data portal, this period coincided with extreme summer meteorological conditions in northern Algeria, characterized by precipitation deficits and unusually high temperatures, which created favorable preconditions for wildfire ignition and spread. All Landsat-8 data were processed using ArcGIS 10.5, including atmospheric correction to reduce the influence of scattering and absorption, Scenes were atmospherically corrected and projection to UTM Zone 31N (WGS84) to ensure spatial consistency across the study area.

2.3 Remote sensing indices

2.3.1 Normalized Difference Vegetation Index (NDVI)

NDVI is a key metric in remote sensing for assessing vegetation cover, density, and health. It was first introduced by Rouse et al. (1973) and is calculated by taking the difference between the near-infrared (NIR) and red (R) reflectance values, divided by their sum, as shown in Equation 1:

$$\mathrm{NDVI} = \frac{(\mathrm{Band\ 5} - \mathrm{Band\ 4})}{(\mathrm{Band\ 5} + \mathrm{Band\ 4})} \tag{1}$$

NDVI values range from –1 to +1. Higher positive values (greater than 0.5) indicate dense and healthy vegetation, while values between 0.2 and 0.5 represent moderate or mixed vegetation. Values between 0 and 0.2 are often associated with barren land, urban areas, or exposed soil, and negative values (below zero) correspond to non-vegetated surfaces such as water, snow, or clouds (Carlson and Ripley 1997; Avdan and Jovanovska 2016; Ekumah et al. 2020).

NDVI is particularly useful for tracking vegetation changes in response to environmental conditions such as droughts, deforestation, or wildfires (Rouse et al. 1973). In post-fire studies, NDVI helps to assess vegetation loss and recovery by comparing pre- and post-fire conditions, as demonstrated in studies across Europe and the Mediterranean (Nolè et al. 2022; Zahabnazouri et al. 2025).

2.3.2 Estimation of Land Surface Temperature (LST)

The estimation of LST from Landsat 8 imagery was carried out in three main steps. First, the raw Digital Numbers (DN) of the thermal bands were converted into spectral radiance using the radiometric rescaling fac
tors provided in the metadata, as shown in Equation 2 (Avdan and Jovanovska 2016):

$$\mathrm{L}_{\lambda} = \mathrm{M}_{\mathrm{L}} \times \mathrm{Q}_{\mathrm{cal}} + \mathrm{A}_{\mathrm{L}} \tag{2}$$

where Lλ represents the spectral radiance, ML is the band-specific multiplicative rescaling factor, Qcal is the quantized pixel value, and AL is the additive rescaling factor provided by the satellite metadata.

Once the spectral radiance is obtained, it is converted into Brightness Temperature (BT) by applying the thermal constants provided in the satellite image metadata. The temperature in degrees Celsius is derived by subtracting the absolute zero (273.15 K) from the brightness temperature, as illustrated in Equation (3) (Cook et al. 2014):

$$\mathrm{BT} = \frac{K_2}{\mathrm{In}\left(\frac{K_1}{L_\lambda}+1\right)} - 273.15 \quad (3)$$

In this equation, K_1 and K_2 are the band-specific thermal conversion constants (with values $K_1 = 774.8853$ and $K_2 = 1321.0789$) (Ru et al. 2021).

Second, the Normalized Difference Vegetation Index (NDVI) is computed to assess the Earth's surface emissivity and the proportion of vegetation. For Landsat 8, NDVI is derived from the reflectance values of Band 5 (Near-Infrared) and Band 4 (Red), as shown in Equation 1. The vegetation proportion (P_v) is calculated using Equation 4 (Rouse et al. 1973):

$$P_v = \left(\frac{\mathrm{NDVI}-\mathrm{NDVI}_{min}}{\mathrm{NDVI}_{max}-\mathrm{NDVI}_{min}}\right)^2 \quad (4)$$

This is followed by the calculation of Land Surface Emissivity (LSE,), which accounts for the emissive properties of the Earth's surface. According to the formula proposed by Sobrino et al. (2004), LSE is estimated based on the vegetation proportion (P_v) as shown in Equation (5):

$$\epsilon = 0.004P_v + 0.986 \quad (5)$$

Once the emissivity is determined, the final step involves computing the LST using the following Equation 6, suggested by Stathopoulou and Cartalis (2007):

$$\mathrm{LST} = \frac{\mathrm{BT}}{1+\left(\frac{\lambda \mathrm{BT}}{\rho}\mathrm{In}(\epsilon\lambda)\right)} \quad (6)$$

Here, $\lambda = 10.895$ µm is the wavelength for Landsat 8's thermal bands, and BT represents the brightness temperature in degrees Celsius (Avdan and Jovanovska 2016). The value ρ is a constant, calculated by the following Equation 7:

$$\rho = \frac{h\times c}{s} = 1.438 \times 10^{-2}\mathrm{Mk} \quad (7)$$

where h is Planck's constant ($6.626 \times {}^{-34}$ Js), s is the Boltzmann constant (1.38×10^{-23} J/K), c is the speed of light (2.998×10^{8} m/s) (Sobrino et al. 2004).

It is important to note that LST is not directly provided by the Landsat sensor but retrieved through these multi-step calculations. The derived LST values are closely related to air temperature and vegetation conditions, where elevated LST indicates reduced evapotranspiration, higher vegetation stress, and increased flammability, thus serving as a useful proxy for wildfire risk (Wasserman and Mueller 2023; Liu et al. 2024).

2.3.3 Normalized Burn Ratio (NBR) and differenced Normalized Burn Ratio (dNBR)

In this research, the NBR was used to identify areas impacted by wildfires (Fernández-Guisuraga et al. 2023), while the dNBR was employed to assess the intensity of burn severity (Maillard et al. 2022; Zhao et al. 2023) (Table 2). Several spectral indices, such as dNBR, have been used in previous studies to assess the effects of fires (Chu et al. 2016). NBR is a widely adopted technique for mapping burned areas before and after fire events (García and Caselles 1991; Key and Benson 2006; Escuin et al. 2008). Similarly, dNBR is frequently used for estimating burn severity based on satellite imagery (Key and Benson 2006; Miller and Thode 2007; Parks et al. 2014).

In this study, both NBR and dNBR indices were calculated to evaluate burn severity. The dNBR was particularly effective for delineating burned areas and classifying the extent of damage (Kurbanov et al. 2022). The NBR was computed for pre- and post-fire images of the Landsat satellite system, specifically using the near-infrared (NIR, Band 5) and mid-infrared (MIR, Band 7) bands, as these bands exhibit significant changes following a fire event (Epting et al. 2005; Roy et al. 2008). NBR is calculated using Equation (8):

$$\mathrm{NBR} = \frac{(\text{Band 5} - \text{Band 7})}{(\text{Band 5} + \text{Band 7})} \tag{8}$$

Subsequently, the dNBR was calculated by subtracting the post-fire NBR from the pre-fire NBR, as shown in Equation (9):

$$dNBR = \mathrm{NBR}_{\text{pre-fire}} - \mathrm{NBR}_{\text{post-fire}} \tag{9}$$

where dNBR = Difference in NBR before and after fires, $\mathrm{NBR}_{\text{pre-fire}}$ = NBR image before fires and $\mathrm{NBR}_{\text{post-fire}}$ = NBR image after fires.

This method allowed for the detection of vegetation changes caused by the fire. The theoretical values for NBR range from −1.0 to +1.0, with lower values typically indicating higher burn severity. The analysis was performed using the Raster Calculator function in ArcGIS 10.5.

Burn severity was classified according to the thresholds proposed by the United States Geological Survey (2016), with dNBR values typically ranging from −2 to +2 and unburned areas having values between −0.10 and +0.10. Specific thresholds were used to classify burn severity levels (Table 2), although these values may vary depending on the geographical context and site characteristics (Key and Benson 2006; Nasery and Kalkan 2020).

Table 2: Differenced Normalized Burn Ratio (dNBR) (Key and Benson 2006; United States Geological Survey 2016).

dNBR range	Burn severity
−0.50 < dNBR < −0.25	High, enhanced regrowth
−0.25 < dNBR < −0.10	Low, enhanced regrowth
−0.10 < dNBR < 0.10	Unburned
0.10 < dNBR < 0.27	Low severity
0.27 < dNBR < 0.44	Moderate-low severity
0.44 < dNBR < 0.66	Moderate-high severity
dNBR > 0.66	High severity

3 Results

3.1 Normalized Difference Vegetation Index (NDVI)

The pre-fire NDVI map (Figure 3a) scene shows strong spatial variation in vegetation density across the study area. High NDVI values (up to 0.87), represented by dark green tones in the eastern and southeastern zones, indicate dense and healthy vegetation, whereas moderate values (0.05 to 0.40) in the central and northern zones suggest sparser vegetation or croplands. Very low values (0.05) in the central-west reflect bare soils or urban areas, providing a baseline for post-fire comparison. In contrast, the post-fire NDVI map (Figure 3b)

Figure 3: NDVI Map for (a) pre-fire and (b) post-fire scenes of the study area. ➤ p. 107

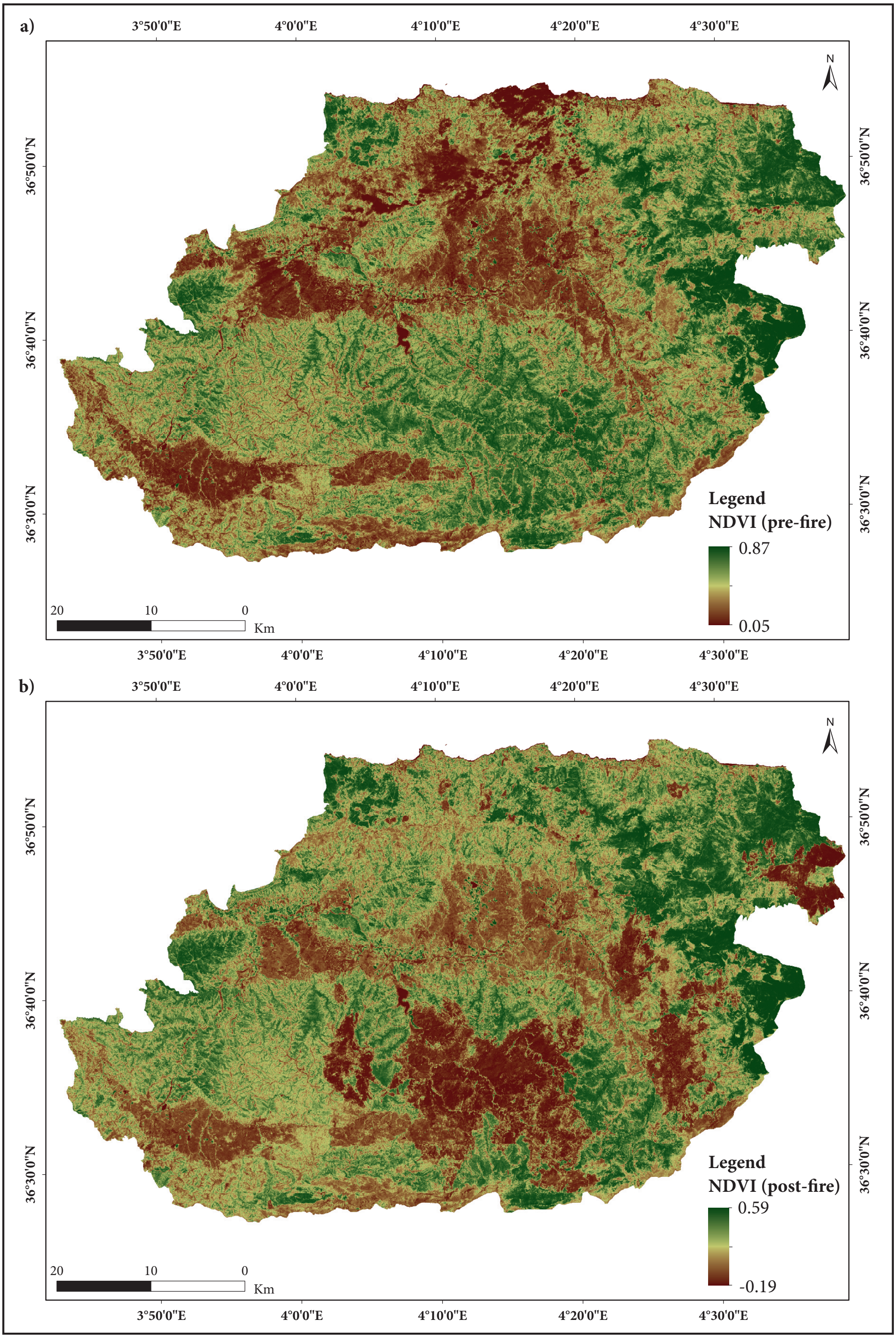
a)
3°50'0"E
4°0'0"E
4°10'0"E
4°20'0"E
4°30'0"E
36°50'0"N
36°40'0"N
36°30'0"N
N
Legend
NDVI (pre-fire)
0.87
0.05
20
10
0
Km
b)
Legend
NDVI (post-fire)
0.59
-0.19

reveals a marked reduction clearly in vegetation cover large portion of the southern and central zones, display low to negative NDVI values (–0.19 to +0.10), highlighting burned or degraded surfaces. Surviving vegetation patches remain mainly in the east and northeast, with NDVI values up to 0.59, indicating areas of lower burn severity.

The widespread decline in NDVI across most of the area suggests significant vegetation loss and ecological disturbance, consistent with wildfire impacts observed in Mediterranean.

3.2 Land Surface Temperature (LST)

The LST analysis reveals notable spatial variations across the Tizi Ouzou region before and after the wildfire event (Figure 4). Pre-fire LST values ranged between 25.92°C to 50.16°C, with higher temperature concentrated in the central and southern parts of the study area, corresponded to the zones that later experienced severe burning as observed in Figure 4a. This correlation implies that elevated pre-fire surface temperatures may have contributed to increasing vegetation dryness and flammability, thereby facilitating the ignition and rapid spread of fire.

Conversely, the northern and northeastern parts of the region displayed relatively lower LST values, represented by blue to turquoise tones. These cooler areas are likely influenced by local environmental factors such as dense vegetation, shading from topographic variation, or higher elevation zones that reduce solar radiation absorption at the surface.

Overall, the spatial distribution of LST prior to the fire event highlights the utility of this parameter as a potential predictive indicator for wildfire risk assessment. Incorporating LST data into fire vulnerability models and early warning systems can significantly enhance preparedness and inform more effective fire management strategies.

Post-fire LST distribution across the Tizi Ouzou region exhibits a distinct thermal pattern when compared to the pre-fire scene. The average LST for the post-fire image is 29.35°C, indicating a general increase in surface temperature following the wildfire event, despite localized variations. Temperature ranges for the post-fire scene were 26.61°C to 46.83°C, as illustrated in Figure 4b.

Higher LST values are mainly concentrated in areas that experienced intense fire damage, particularly in the central and southern parts of the study area. These zones appear in red to orange hues and reflect residual surface heating associated with the loss of vegetation cover and changes in surface albedo. The increase in LST in burned regions is consistent with findings from previous studies, which report that burned surfaces can be significantly warmer – up to 7.6°C higher than unburned zones, and even more than 10°C in high burn severity areas (Vlassova et al. 2014).

In contrast, areas in the northern and northeastern regions, which were either unaffected or less impacted by the fire, demonstrate relatively lower surface temperatures (shown in blue and green shades). This suggests that vegetation and soil conditions in unburned zones continued to moderate heat retention and reflectance, resulting in cooler post-fire LST values.

Overall, the observed LST increase in burned areas highlights the impact of wildfires on surface energy balance and emphasizes the role of LST as a valuable post-disturbance diagnostic tool in fire-affected landscapes.

3.3 Correlation between NDVI and LST

The scatterplots provided in Figure 5 illustrate the relationship between NDVI and LST both before and after the fire event. Before the fire, the data shows a relatively strong negative correlation between NDVI and LST, with an R^2 value of 0.5668, indicating that healthy vegetation significantly contributed to surface cooling. This pattern is consistent with several studies which confirmed that areas with dense vegetation exhibit lower surface temperatures due to shading effects and evapotranspiration (Vlassova et al. 2014). Such findings affirm the important role vegetation plays in regulating local microclimates. According to Yuan and Bauer (2007), higher NDVI values are typically associated with lower LST in forested ecosystems, emphasizing vegetation's critical cooling function.

Figure 4: LST Map for (a) pre-fire and (b) post-fire scenes of the study area. ➤ p. 109

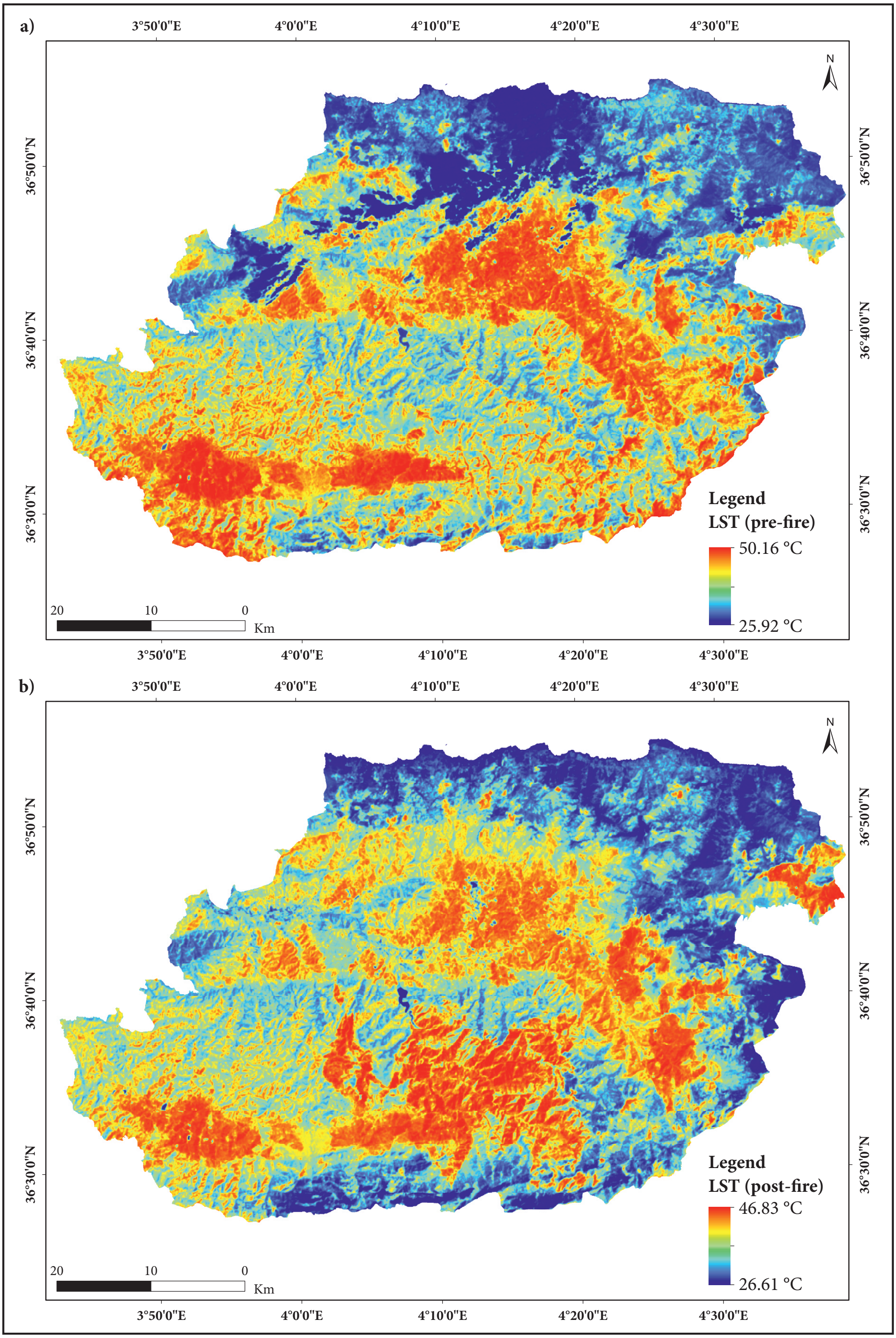
a)
3°50'0"E
4°0'0"E
4°10'0"E
4°20'0"E
4°30'0"E
36°50'0"N
36°40'0"N
36°30'0"N
N
Legend
LST (pre-fire)
50.16 °C
25.92 °C
20
10
0
Km
b)
Legend
LST (post-fire)
46.83 °C
26.61 °C

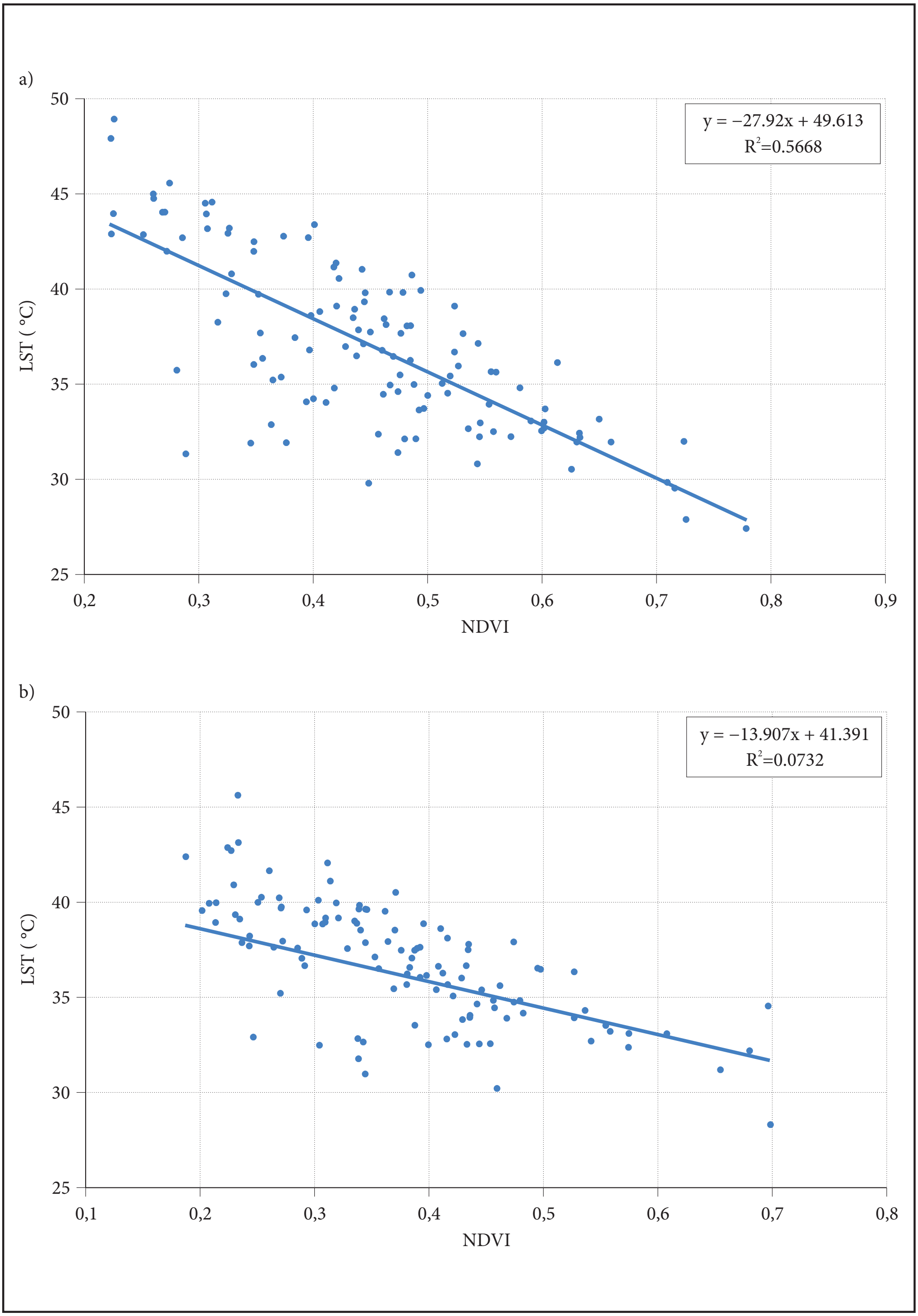

Figure 5: Correlation Matrix for NDVI-LST relationship (a) before and (b) after the wildfire event.

After the fire, the correlation between NDVI and LST weakens significantly, with an R^2 value dropping to 0.0752, this pattern highlights how fire disrupts the natural land-atmosphere interactions by removing vegetative cover, leading to hotter surface conditions. Similar results were observed by Chuvieco et al. (2019), who reported that post-fire landscapes maintain elevated LST due to the absence of vegetation, which increases soil heat absorption. The sharp reduction in the strength of the NDVI–LST relationship after the fire event indicates that vegetation loss severely alters land surface thermal properties. Over time, if vegetation regenerates, one would expect the correlation to gradually become stronger again, as shown by studies monitoring post-fire recovery (Digavinti and Manikiam 2021).

3.4 Normalized Burn Ratio (NBR)

The incorporation of both pre- and post-fire NBR indices into fire risk mapping plays a pivotal role in enhancing our understanding and anticipation of wildfire dynamics. NBR, derived from remote sensing techniques, serves as an essential metric for evaluating the intensity of vegetation damage resulting from fires, offering vital information on alterations within the landscape. Evaluating NBR values before and after fire incidents allows for a detailed examination of wildfire susceptibility patterns.

The pre-fire NBR on 30th June, 2021 (Figure 6a) provides a reference point for assessing vegetation health prior to fire occurrence. Lower pre-fire NBR readings may suggest existing vegetation stress or sparse coverage, potentially serving as indicators of higher ignition likelihood. Conversely, the post-fire NBR on 30th September, 2021 illustrates the degree of vegetation degradation caused by fire, highlighting zones with pronounced ecological transformations. When both sets of data are compared (Figure 6b), it becomes possible to pinpoint regions that underwent significant vegetation loss, thus identifying zones of critical impact. Elevated post-fire NBR values are often linked with severe burn damage, signifying regions at greater risk, while lower values may reflect milder impacts or areas where vegetation persisted post-fire. Furthermore, the analysis of NBR values showed that, during the pre-fire phase, readings ranged between −0.58, which corresponds to barren or non-vegetated surfaces, and +0.25, indicative of healthy, dense vegetation. In the post-fire phase, values ranged from −0.74 to +0.26 (Figure 6), illustrating the varying degrees of fire-induced changes across the study area.

The temporal comparison of NBR values, capturing both pre- and post-event conditions, supports a more dynamic and accurate interpretation of fire vulnerability. This method enhances mapping precision by accounting for landscape alterations driven by fire activity. Utilizing both pre- and post-NBR datasets in fire susceptibility assessments enables better identification of areas susceptible to intense vegetation loss and facilitates the evaluation of fire aftermath effects.This dual-index approach not only improves the reliability of fire risk assessments but also supports more informed decisions regarding mitigation planning, resource distribution, and sustainable land management.

3.5 Differenced Normalized Burn Ratio (dNBR)

Based on the dNBR values, five distinct burn severity classes were identified: unburned, low severity, moderate-low severity, moderate-high severity, and high severity. These classifications were used to generate the burn severity map (Figure 7). According to the dNBR classification (Table 3), 6.66% (24,684.66 ha) of the study area was categorized as high severity, 14.89% (55,200.69 ha) as moderate-high severity, 25.48% (94,491.81 ha) as moderate-low severity, and 34.26% (127,044.09 ha) as low severity. In addition, 14.97% (55,537.92 ha) of the land remained unburned, while vegetation regrowth was detected in 1.93% (7158.96 ha) as low regrowth and 1.81% (6700.05 ha) as high regrowth zones. Higher dNBR values were associated with severe fire damage, while lower values indicated better preserved vegetation. A related study by Guehaz and Sivakumar (2023) examined the forest fire that occurred on 5th July, 2021 in Khenchela province, Algeria, using space-borne remote sensing data. Their analysis, based on Landsat-8 and Sentinel-2 imagery, applied both dNBR and RdNBR indices to evaluate burn severity across affected municipalities such as Tamza, Chelia, Elhamma, and Bouhmama. According to their dNBR-based classification, 1.21% (1825.11 ha) of

Figure 6: NBR of (a) pre-fire and (b) post-fire scenes of the study area. ➤ p. 112

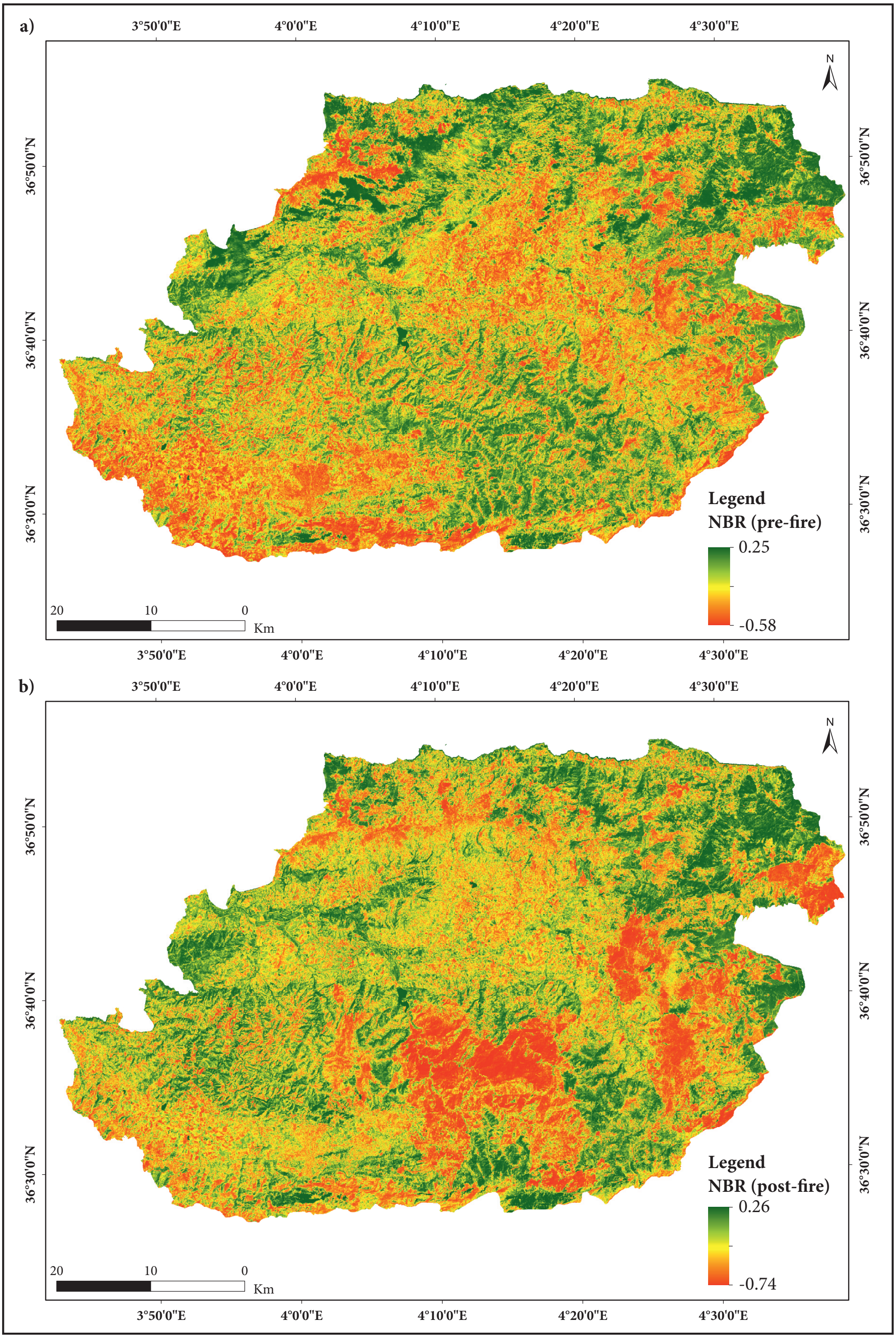
a)
3°50'0"E
4°0'0"E
4°10'0"E
4°20'0"E
4°30'0"E
36°50'0"N
36°40'0"N
36°30'0"N
N
Legend
NBR (pre-fire)
0.25
-0.58
20
10
0
Km
b)
3°50'0"E
4°0'0"E
4°10'0"E
4°20'0"E
4°30'0"E
36°50'0"N
36°40'0"N
36°30'0"N
N
Legend
NBR (post-fire)
0.26
-0.74
20
10
0
Km

the area experienced high severity burns, 2.54% (3843.54 ha) suffered moderate-high severity, 2.59% (3927.97 ha) was classified under moderate-low severity, and 6.51% (9864.45 ha) experienced low severity. The most affected municipalities are Ouacifs, Ath Yenni, Larba y Nath Irathen, and Ain El Hammam. These findings were critical for mapping the spatial extent and intensity of fire impact (Guehaz and Sivakumar 2023).

Table 3: Differenced Normalized Burn Ratio (dNBR) thresholds proposed by the United States Geological Survey (2016).

Burn severity level	Burned area (ha)	Burned area (%)
High, enhanced regrowth	6700.05	1.81
Low, enhanced regrowth	7158.96	1.93
Unburned	55537.92	14.97
Low severity	127044.09	34.26
Moderate-low severity	94491.81	25.48
Moderate-high severity	55200.69	14.89
High severity	24684.66	6.66

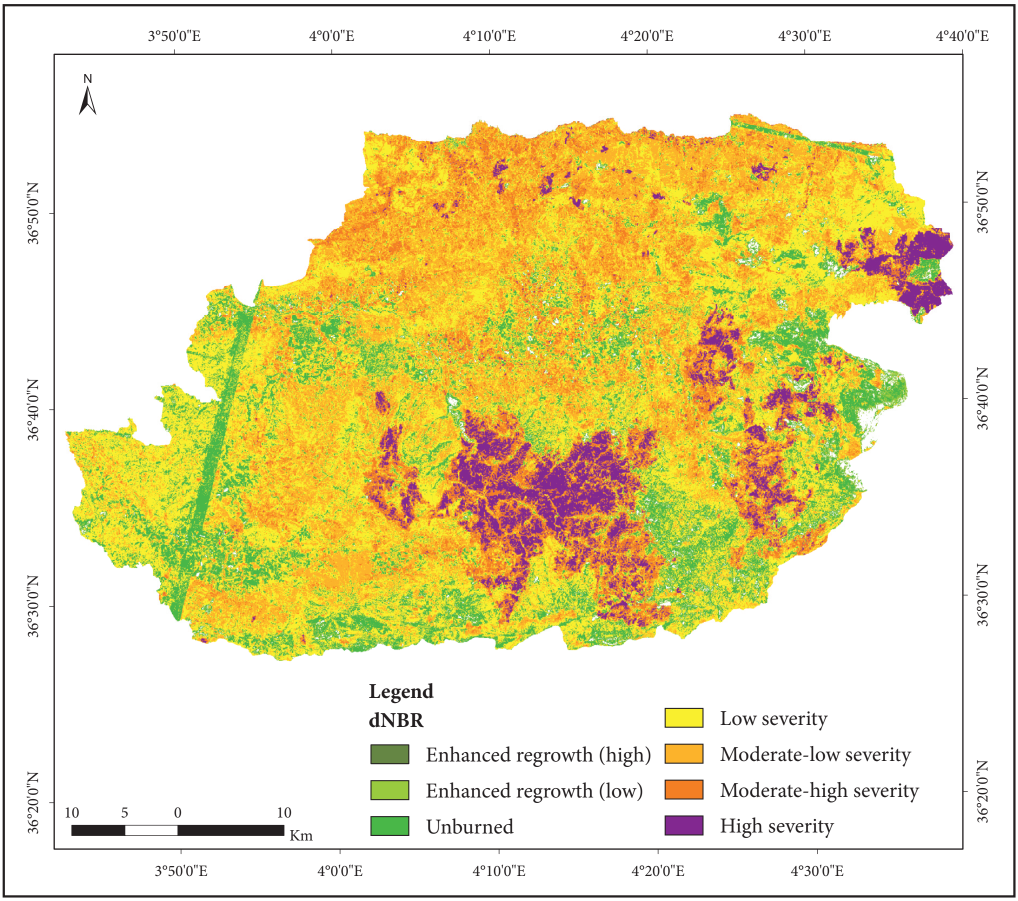

Figure 7: dNBR based burn severity map of the study area.

Furthermore, their study compared these results with those obtained using the relativized dNBR (RdNBR), which showed variations in severity levels: low (9.442 kha), moderate-low (3.077 kha), moderate-high (3.953 kha), and high severity (2.654 kha). The authors concluded that RdNBR provided a more accurate and reliable estimate of fire severity than dNBR alone, particularly due to its better sensitivity across heterogeneous landscapes. In comparison, the current study assessing the 2021 wildfire in Tizi Ouzou revealed a greater extent of burn severity.

This comparative analysis underscores the greater intensity and spatial extent of fire damage in Tizi Ouzou relative to Khenchela. While Khenchela showed only 1.21% under high severity, Tizi Ouzou high severity class was over five times larger. Such differences could stem from variations in vegetation cover, topography, and fire behavior, highlighting the importance of region-specific remote sensing assessments for effective post-fire recovery strategies.

4 Discussion

Our results underscore the critical role of multispectral remote sensing – particularly Landsat-derived indices – in accurately mapping forest fire severity and assessing post-fire ecological impacts. Consistent with global best practices, the dNBR remains a core metric for delineating burn severity across diverse forest types (Key and Benson 2006; Tran et al. 2018; Chuvieco et al. 2019). In the context of Mediterranean ecosystems, dNBR has repeatedly proven effective due to its sensitivity to changes in vegetation and soil reflectance in the shortwave infrared range. Our findings confirm this pattern, with dNBR outper forming NDVI in distinguishing high-severity burn zones in Tizi Ouzou.

Several studies affirm that no single index universally outperforms others; rather, the effectiveness of indices varies depending on forest type and fire regime. For instance, dNBR is often more responsive in resprouting forests, while dNDVI and dNDWI may yield better accuracy in seeder-dominated landscapes (Lentile et al. 2006; Miller and Thode 2007; Tran et al. 2018). This variability was also observed in our study: while dNBR captured the most intense burn zones, NDVI proved more useful in detecting early vegetation regrowth. This aligns with Zennir and Khallef (2023), who also adopted a multi-index approach in the Beni Salah Forest, suggesting that integrating indices offers a more robust characterization of fire effects.

In their analysis, Zennir and Khallef (2023) relied on Sentinel-2 data to detect severe burn zones, while our use of Landsat-8 demonstrated that comparable results can be achieved at a broader regional scale. This indicates that Landsat imagery, despite its coarser resolution, remains highly suitable for large-scale fire severity mapping in Algeria. Similarly, Chuvieco et al. (2018) highlighted the importance of combining multiple indices and leveraging both pre- and post-fire imagery. Our results support this approach, as the integration of NDVI and dNBR enabled us not only to delineate burned areas but also to quantify vegetation loss and partial recovery.

A more recent contribution by Sabljić et al. (2025) confirmed the value of spectral differencing in Mediterranean ecosystems. Their Sentinel-2 analysis captured both immediate fire impacts and recovery trends, findings that parallel our own NDVI-based monitoring of post-fire regrowth in Tizi Ouzou. Likewise, Zikiou et al. (2024) showed that areas with dense suffered more intense damage, a relationship we also observed: zones with higher pre-fire NDVI and elevated LST values in our study area corresponded to higher dNBR severity classes.

These findings reinforce the importance of integrating remote sensing and machine learning technologies in fire risk assessment and management, particularly in fire-prone regions like Algeria. Our findings further highlight the suitability of Landsat-8 OLI imagery, given its spatial and spectral resolution, for detecting burn severity and vegetation degradation (Veraverbeke et al. 2012; Roy et al. 2014). Temporal NDVI analysis in our study clearly demonstrated vegetation health loss post-fire, confirming remote sensing's role in ecological monitoring (De Santis and Chuvieco 2009). NDVI has shown particular utility in tracking regrowth trajectories over time, allowing researchers to monitor ecosystem resilience and degradation trends (Koutsias et al. 2004; Gitas et al. 2012).

Finally, GIS-based mapping of fire severity proved critical for guiding land management and restoration efforts. While earlier works (Keeley 2009; Fernandes 2013) highlighted the value of spatial data for fire policy, our study demonstrates its practical application in Tizi Ouzou, where severity maps can inform targeted reforestation and fire prevention strategies.

5 Conclusion

This study demonstrates the effectiveness of remote sensing and geospatial analysis in assessing forest fire severity and understanding post-fire ecological transformations in the Tizi Ouzou region during the 2021 wildfires. The integration of Landsat-8 imagery with atmospheric data and GIS-based mapping methods underscores the robustness of these tools in fire monitoring and management. The NDVI results highlighted a marked decline in vegetation cover, clearly capturing the loss of biomass, while the NBR and dNBR indices proved particularly effective in quantifying burn severity and delineating the spatial distribution of damage across different land cover types. In addition, the analysis of LST provided complementary insights into the thermal impacts of the fires, confirming areas of ecological stress and intensifying the interpretation of burn severity. Collectively, these findings underscore the capacity of geospatial technologies to generate rapid, reliable, and spatially explicit information to support wildfire monitoring and environmental management in Mediterranean regions. Nevertheless, some limitations were encountered. The use of medium-resolution Landsat 8 imagery constrained the level of detail in fire severity mapping, while the absence of extensive ground-truth data restricted the validation of the obtained results. Furthermore, vegetation indices may be influenced by seasonal agricultural practices, which can occasionally interfere with accurate fire-related classification. Future research should aim to integrate higher-resolution imagery (e.g., Sentinel-2 or PlanetScope), field-based validation campaigns, and advanced techniques such as multi-sensor fusion and machine learning approaches. Long-term monitoring of vegetation regrowth and resilience after wildfires would also enhance understanding of ecosystem recovery dynamics. Such improvements will contribute to the development of more effective strategies for fire risk assessment, ecosystem restoration, and sustainable land management in Algeria and similar Mediterranean environments.

RESEARCH DATA: For information on the availability of research data related to the study, please visit the article webpage: https://doi.org/10.3986/AGS.14459

6 References

Ammiche, S., Oumezzaouche, N. 2018: Valorisation des produits forestiers non ligneux dans la wilaya de Tizi-Ouzou: cas de la forêt des Béni Ghobri. *Ph.D. thesis*. Université Mouloud Mammeri.

Arfa, A. M. T., Benderradji, M. E. H., Saint-Gérand, T., Alatou, D. 2019: Cartographie du risque feu de forêt dans le Nord-est algérien: cas de la wilaya d'El Tarf. *Cybergeo: European Journal of Geography*. https://doi.org/10.4000/cybergeo.32304

Avdan, U., Jovanovska, G. 2016: Algorithm for automated mapping of land surface temperature using LANDSAT 8 satellite data. *Journal of Sensors* 2016-1. https://doi.org/10.1155/2016/1480307

Belgherbi, B., Benabdeli, K., Mostefai, K. 2018: Mapping the risk of forest fires in Algeria: application of the forest of Guetarnia in Western Algeria. *Ekológia* 37-3. https://doi.org/10.2478/eko-2018-0022

Brewer, C. K., Winne, J. C., Redmond, R. L., Opitz, D. W., Mangrich, M. V. 2005: Classifying and mapping wildfire severity. *Photogrammetric Engineering & Remote Sensing* 11. https://doi.org/10.14358/PERS.71.11.1311

Cansler, C. A., McKenzie, D. 2012: How robust are burn severity indices when applied in a new region? Evaluation of alternate field-based and remote-sensing methods. *Remote Sensing* 4-2. https://doi.org/10.3390/rs4020456

Carlson, T. N., Ripley, D. A. 1997: On the relation between NDVI, fractional vegetation cover, and leaf area index. *Remote Sensing of Environment* 62-3. https://doi.org/10.1016/S0034-4257(97)00104-1

Castro-Melgar, I., Tsagkou, A., Zacharopoulou, M., Basiou, E., Athinelis, I., Katris, E. A., Kalavrezou, I. E. et al. 2025: Wildfires during early summer in Greece (2024): Burn severity and land use dynamics through Sentinel-2 data. *Forests* 16-2. https://doi.org/10.3390/f16020268

Chu, T., Guo, X., Takeda, K. 2016: Remote sensing approach to detect post-fire vegetation regrowth in Siberian boreal larch forest. *Ecological Indicators* 62. https://doi.org/10.1016/j.ecolind.2015.11.026

Chuvieco, E., Lizundia-Loiola, J., Pettinari, M. L., Ramo, R., Padilla, M., Tansey, K., Mouillot, F. et al. 2018: Generation and analysis of a new global burned area product based on MODIS 250 m reflectance bands and thermal anomalies. *Earth System Science Data* 10-4. https://doi.org/10.5194/essd-10-2015-2018

Chuvieco, E., Mouillot, F., Van der Werf, G. R., San Miguel, J., Tanase, M., Koutsias, N., García, M. et al. 2019: Historical background and current developments for mapping burned area from satellite Earth observation. *Remote Sensing of Environment* 225. https://doi.org/10.1016/j.rse.2019.02.013

Cocke, A. E., Fulé, P. Z., Crouse, J. E. 2005: Comparison of burn severity assessments using Differenced Normalized Burn Ratio and ground data. *International Journal of Wildland Fire* 14-2. https://doi.org/10.1071/WF04010

Conservation des forêts Tizi Ouzou 2021: Bilan annuel des incendies de forêt, Campagne 2021. *Technical report*.

Cook, M., Schott, J. R., Mandel, J., Raqueno, N. 2014: Development of an operational calibration methodology for the Landsat thermal data archive and initial testing of the atmospheric compensation component of a Land Surface Temperature (LST) Product from the archive. *Remote Sensing* 6-11. https://doi.org/10.3390/rs61111244

De Santis, A., Chuvieco, E. 2009: GeoCBI: A modified version of the Composite Burn Index for the initial assessment of the short-term burn severity from remotely sensed data. *Remote Sensing of Environment* 113-3. https://doi.org/10.1016/j.rse.2008.10.011

Digavinti, J., Manikiam, B. 2021: Satellite monitoring of forest fire impact and regeneration using NDVI and LST. *Journal of Applied Remote Sensing* 15-4. https://doi.org/10.1117/1.JRS.15.042412

Direction Générale des Forêts 2021: Bilan des incendies de forêts en Algérie. Ministère de l'Agriculture et du Développement Rural. *Report*.

Dupuy, J. L., Fargeon, H., Martin-StPaul, N., Pimont, F., Ruffault, J., Guijarro, M., Fernandes, P. et al. 2020: Climate change impact on future wildfire danger and activity in southern Europe: A review. *Annals of Forest Science* 77-2. https://doi.org/10.1007/s13595-020-00933-5

Durlević, U., Srejić, T., Valjarević, A., Aleksova, B., Deđanski, V., Vujović, F., Lukić, T. 2025: GIS-based spatial modeling of soil erosion and wildfire susceptibility ssing VIIRS and Sentinel-2 data: A case study of Šar Mountains National Park, Serbia. *Forests* 16-3. https://doi.org/10.3390/f16030484

Ekumah, B., Armah, F. A., Afrifa, E. K., Aheto, D. W., Odoi, J. O., Afitiri, A. R. 2020: Geospatial assessment of ecosystem health of coastal urban wetlands in Ghana. *Ocean & Coastal Management* 193. https://doi.org/10.1016/j.ocecoaman.2020.105226

Epting, J., Verbyla, D. Sorbel, B. 2005: Evaluation of remotely sensed indices for assessing burn severity in interior Alaska using Landsat TM and ETM+. *Remote Sensing of Environment* 96-3,4. https://doi.org/10.1016/j.rse.2005.03.002

Escuin, S., Navarro, R. Fernández, P. 2008: Fire severity assessment by using NBR (Normalized Burn Ratio) and NDVI (Normalized Difference Vegetation Index) derived from LANDSAT TM/ETM images. *International Journal of Remote Sensing* 29-4. https://doi.org/10.1080/01431160701281072

Fernandes, P. M. 2013: Fire-smart management of forest landscapes in the Mediterranean basin under global change. *Landscape and Urban Planning* 110. https://doi.org/10.1016/j.landurbplan.2012.10.014

Fernández-Guisuraga, J. M., Calvo, L., Quintano, C., Fernández-Manso, A., Fernandes, P. M. 2023: Fractional vegetation cover ratio estimated from radiative transfer modeling outperforms spectral indices to assess fire severity in several Mediterranean plant communities. *Remote Sensing of Environment* 290. https://doi.org/10.1016/j.rse.2023.113542

Ganteaume, A., Barbero, R. 2019: Contrasting large fire activity in the French Mediterranean. *Natural Hazards and Earth System Sciences* 19-5. https://doi.org/10.5194/nhess-19-1055-2019

García, M. L., Caselles, V. 1991: Mapping burns and natural reforestation using Thematic Mapper data. *Geocarto International* 6-1. https://doi.org/10.1080/10106049109354290

Gitas, I., Mitri, G., Veraverbeke, S., Polychronaki, A. 2012: Advances in remote sensing of post-fire vegetation recovery monitoring – A review. In: Remote Sensing of Biomass – Principles and Applications. IntechOpen. https://doi.org/10.5772/20571

Guehaz, R., Sivakumar, V. 2023: A case study about the forest fire occurred on 05 July 2021 over Khenchela province, Algeria, using space-borne remote sensing. *Frontiers in Remote Sensing* 4. https://doi.org/10.3389/frsen.2023.1289963

Harris, S., Veraverbeke, S., Hook, S. 2011: Evaluating spectral indices for assessing fire severity in chaparral ecosystems (Southern California) using MODIS/ASTER (MASTER) airborne simulator data. *Remote sensing* 3-11. https://doi.org/10.3390/rs3112403

Keeley, J. E. 2009: Fire intensity, fire severity and burn severity: A brief review and suggested usage. *International Journal of Wildland Fire* 18-1. https://doi.org/10.1071/WF07049

Key, C. H., Benson, N. C. 2006: Landscape assessment (LA). In: FIREMON: Fire effects monitoring and inventory system. *General technical report*. U.S. Department of Agriculture, Forest Service, Rocky Mountain Research Station.

Kouachi, M. E., Khairoun, A., Moghli, A., Rahmani, S., Mouillot, F., Baeza, M. J., Moutahir, H. 2024: Forty-year fire history reconstruction from Landsat data in Mediterranean ecosystems of Algeria following international standards. *Remote sensing* 16-13. https://doi.org/10.3390/rs16132500

Koutsias, N., Kalabokidis, K. D. Allgöwer, B. 2004: Fire occurrence patterns at landscape level: Beyond positional accuracy of ignition points with kernel density estimation methods. *Natural Resource Modeling* 17-4. https://doi.org/10.1111/j.1939-7445.2004.tb00141.x

Koutsias, N., Karamitsou, A., Nioti, F., Coutelieris, F. 2022: Assessment of fire regimes and post-fire evolution of burned areas with the dynamic time warping method on time series of satellite images – setting the methodological framework in the Peloponnese, Greece. *Remote Sensing* 14-20. https://doi.org/10.3390/rs14205237

Kurbanov, E., Vorobev, O., Lezhnin, S., Sha, J., Wang, J., Li, X., Cole, J. et al. 2022: Remote sensing of forest burnt area, burn severity, and post-fire recovery: A review. *Remote Sensing* 14-19. https://doi.org/10.3390/rs14194714

Lahmar, B., Akakba, A. 2024: Forest fire detection based on earlier pre-fire conditions using analysis hierarchic process (AHP) in a semi-arid climate. A case study: Belezma National Park, Algeria. *Acta Geographica Lodziensia* 114. https://doi.org/10.26485/AGL/2024/114/3

Lentile, L. B., Holden, Z. A., Smith, A. M., Falkowski, M. J., Hudak, A. T., Morgan, P., Lewis, S. A. et al. 2006: Remote sensing techniques to assess active fire characteristics and post-fire effects. *International Journal of Wildland Fire* 15-3. https://doi.org/10.1071/WF05097

Liu, J., Wang, Y., Guo, H., Lu, Y., Xu, Y., Sun, Y., Gan, W. et al. 2024: Spatial and temporal patterns and driving factors of forest fires based on an optimal parameter-based geographic detector in the Panxi region, Southwest China. *Fire Ecology* 20-1. https://doi.org/10.1186/s42408-024-00257-z

Lovreglio, R., Leone, V., Giaquinto, P., Notarnicola, A. 2010: Wildfire cause analysis: Four case-studies in southern Italy. *iForest-Biogeosciences and Forestry* 3-1. https://doi.org/10.3832/ifor0521-003

Lukić, T., Marić, P., Hrnjak, I., Gavrilov, M. B., Mladjan, D., Zorn, M., Komac, B. et al. 2017: Forest fire analysis and classification based on a Serbian case study. *Acta geographica Slovenica* 57-1. https://doi.org/10.3986/AGS.918

Maillard, O., Flores-Valencia, M., Michme, G., Coronado, R., Bachfischer, M., Azurduy, H., Vides-Almonacid, R. et al. 2022: Phenology patterns and postfire vegetation regeneration in the Chiquitania region of Bolivia using Sentinel-2. *Fire* 5-3. https://doi.org/10.3390/fire5030070

Meddour-Sahar, O., Derridj, A. 2010: Le risque d'incendie de forêt: évaluation et cartographie. *Science et changements planétaires/Sécheresse* 21-3.

Miller, J. D., Thode, A. E. 2007: Quantifying burn severity in a heterogeneous landscape with a relative version of the delta Normalized Burn Ratio (dNBR). *Remote Sensing of Environment* 109-1. https://doi.org/10.1016/j.rse.2006.12.006

Mouillot, F., Ratte, J. P., Joffre, R., Moreno, J. M., Rambal, S. 2003: Some determinants of the spatio-temporal fire cycle in a Mediterranean landscape (Corsica, France). *Landscape Ecology* 18. https://doi.org/10.1023/B:LAND.0000004182.22525.a9

Nasery, S., Kalkan, K. 2020: Burn area detection and burn severity assessment using Sentinel 2 MSI data: The case of Karabağlar district, İzmir/Turkey. *Turkish Journal of Geosciences* 1-2.

Nolè, A., Rita, A., Spatola, M. F., Borghetti, M. 2022: Biogeographic variability in wildfire severity and post-fire vegetation recovery across the European forests via remote sensing-derived spectral metrics. *Science of The Total Environment* 823. https://doi.org/10.1016/j.scitotenv.2022.153807

Oliveira, S., Oehler, F., San-Miguel-Ayanz, J., Camia, A., Pereira, J. M. 2012: Modeling spatial patterns of fire occurrence in Mediterranean Europe using Multiple Regression and Random Forest. *Forest Ecology and Management* 275. https://doi.org/10.1016/j.foreco.2012.03.003

Parks, S. A., Dillon, G. K., Miller, C. 2014: A new metric for quantifying burn severity: the relativized burn ratio. *Remote Sensing* 6-3. https://doi.org/10.3390/rs6031827

Rahmani, S., Benmassoud, H. 2019: Modelling of forest fire risk spatial distribution in the region of Aures, Algeria. *Geoadria* 24-2. https://doi.org/10.15291/geoadria.2846

Rouse, J. W., Haas, R. H., Schell, J. A., Deering, D. W. 1973: Monitoring the vernal advancement and retrogradation (green wave effect) of natural vegetation. Progress Report RSC 1978-2. *Technical Report.* NASA.

Roy, D. P., Boschetti, L., Justice, C. O., Ju, J. 2008: The collection 5 MODIS burned area product – Global evaluation by comparison with the MODIS active fire product. *Remote Sensing of Environment* 112-9. https://doi.org/10.1016/j.rse.2008.05.013

Roy, D. P., Wulder, M. A., Loveland, T. R., Woodcock, C. E., Allen, R. G., Anderson, M. C., Helder, D. et al. 2014: Landsat-8: Science and product vision for terrestrial global change research. *Remote Sensing of Environment* 145. https://doi.org/10.1016/j.rse.2014.02.001

Ru, C., Duan, S. B., Jiang, X. G., Li, Z. L., Jiang, Y., Ren, H., Leng, P. et al. 2021: Land surface temperature retrieval from Landsat 8 thermal infrared data over urban areas considering geometry effect: Method and application. *IEEE Transactions on geoscience and remote sensing* 60. https://doi.org/10.1109/TGRS.2021.3088482

Sabljić, L., Perić, Z. M., Bajić, D., Marković, S. B., Adžić, D., Lukić, T. 2025: Advancing wildfire monitoring: remote sensing techniques and applications in the Sana River Basin, Bosnia and Herzegovina. *Natural Hazards* 1-40. https://doi.org/10.1007/s11069-025-07518-3

Sahar, O., Hamel, H., Meddour, R. 2020: Etude des grands feux de forêts en Algérie: Cas de la wilaya de Tizi Ouzou. *Geo-Eco-Trop* 44-3.

San-Miguel-Ayanz, J., Durrant, T., Boca, R., Maianti, P., Libertá, G., Artés-Vivancos, T., Oom, D. et al. 2022: Advance report on wildfires in Europe, Middle East and North Africa 2021. *Technical report*. Publications Office of the European Union. https://doi.org/10.2760/039729

Sobrino, J. A., Jiménez-Muñoz, J. C., Paolini, L. 2004: Land surface temperature retrieval from LANDSAT TM 5. *Remote Sensing of Environment* 90-4. https://doi.org/10.1016/j.rse.2004.02.003

Stathopoulou, M., Cartalis, C. 2007: Daytime urban heat islands from Landsat ETM+ and Corine land cover data: An application to major cities in Greece. *Solar Energy* 81-3. https://doi.org/10.1016/j.solener.2006.06.014

Stefanidis, S., Alexandridis, V., Spalevic, V., Mincato, R. L. 2022: Wildfire effects on soil erosion dynamics: The case of 2021 megafires in Greece. *Agriculture & Forestry* 68-2. https://doi.org/10.17707/AgricultForest.68.2.04

Tran, B. N., Tanase, M. A., Bennett, L. T., Aponte, C. 2018: Evaluation of spectral indices for assessing fire severity in Australian temperate forests. *Remote Sensing* 10-11. https://doi.org/10.3390/rs10111680

Turco, M., Jerez, S., Augusto, S., Tarín-Carrasco, P., Ratola, N., Jiménez-Guerrero, P., Trigo, R. M. 2019: Climate drivers of the 2017 devastating fires in Portugal. *Scientific Reports* 9-1. https://doi.org/10.1038/s41598-019-50281-2

United States Geological Survey 2016: Landsat – Earth Observation Satellites. Fact sheet. https://doi.org/10.3133/fs20153081

Veraverbeke, S., Hook, S., Hulley, G. 2012: An alternative spectral index for rapid fire severity assessments. *Remote Sensing of Environment* 123. https://doi.org/10.1016/j.rse.2012.02.025

Veraverbeke, S., Lhermitte, S., Verstraeten, W. W., Goossens, R. 2010: The temporal dimension of differenced Normalized Burn Ratio (dNBR) fire/burn severity studies: The case of the large 2007 Peloponnese wildfires in Greece. *Remote Sensing of Environment* 114-11. https://doi.org/10.1016/j.rse.2010.05.029

Vlassova, L., Pérez-Cabello, F., Mimbrero, M. R., Llovería, R. M., García-Martín, A. 2014: Analysis of the relationship between land surface temperature and wildfire severity in a series of Landsat images. *Remote Sensing* 6-7. https://doi.org/10.3390/rs6076136

Vujović, F., Valjarević, A., Vila-Subirós, J., Šiljeg, A., Lukić, T. 2024: Geospatial modeling of wildfire susceptibility on a national scale in Montenegro: A comparative evaluation of F-AHP and FR methodologies. *Open Geosciences* 16-1. https://doi.org/10.1515/geo-2022-0694

Wasserman, T. N., Mueller, S. E. 2023: Climate influences on future fire severity: A synthesis of climate-fire interactions and impacts on fire regimes, high-severity fire, and forests in the western United States. *Fire Ecology* 19-1. https://doi.org/10.1186/s42408-023-00200-8

Wendt, C. K., Beringer, J., Tapper, N. J., Hutley, L. B. 2007: Local boundary-layer development over burnt and unburnt tropical savanna: An observational study. *Boundary-Layer Meteorology* 124. https://doi.org/10.1007/s10546-006-9148-3

Yuan, F., Bauer, M. E. 2007: Comparison of impervious surface area and normalized difference vegetation index as indicators of surface urban heat island effects in Landsat imagery. *Remote Sensing of Environment* 106-3. https://doi.org/10.1016/j.rse.2006.09.003

Zahabnazouri, S., Belmont, P., David, S., Wigand, P. E., Elia, M., Capolongo, D. 2025: Detecting burn severity and vegetation recovery after fire using dNBR and dNDVI indices: Insight from the Bosco Difesa Grande, Gravina in Southern Italy. *Sensors* 25-10. https://doi.org/10.3390/s25103097

Zennir, R., Khallef, B. 2023: Forest fire area detection using Sentinel-2 data: Case of the Beni Salah national forest‑Algeria. *Journal of Forest Science* 69-1. https://doi.org/10.17221/50/2022-JFS

Zhao, Y., Huang, Y., Sun, X., Dong, G., Li, Y., Ma, M. 2023: Forest fire mapping using multi-source remote sensing data: A case study in Chongqing. *Remote Sensing* 15-9. https://doi.org/10.3390/rs15092323

Zikiou, N., Rushmeier, H., Capel, M. I., Kandakji, T., Rios, N., Lahdir, M. 2024: Remote sensing and machine learning for accurate fire severity mapping in northern Algeria. *Remote Sensing* 16-9. https://doi.org/10.3390/rs16091517